

Deflection enhancement of ferrite magnetic core-based microactuator

Roer Eka Pawinanto¹, Budi Mulyanti^{2,3}, Jahril Nur Fauzan⁴, Ayub Subandi^{5,6}, Lilik Hasanah⁷, M. Assadillah Pangestu⁴, Jumril Yunas⁶

¹Study Program of Industrial Automation Engineering Education and Robotics, Faculty of Engineering Education and Industry, Universitas Pendidikan Indonesia, Bandung, Indonesia

²Study Program of Electrical Engineering, Faculty of Engineering Education and Industry, Universitas Pendidikan Indonesia, Bandung, Indonesia

³Technical and Vocational Education and Training Research Center, Universitas Pendidikan Indonesia, Bandung, Indonesia

⁴Study Program of Electrical Engineering Education, Faculty of Engineering Education and Industry, Universitas Pendidikan Indonesia, Bandung, Indonesia

⁵Study Program of Computer Systems, Faculty of Engineering and Computer Science, Universitas Komputer Indonesia, Bandung, Indonesia

⁶Institute of Microengineering and Nanoelectronics, Universiti Kebangsaan Malaysia, Bangi, Malaysia

⁷Study Program of Physics, Faculty of Mathematics and Natural Sciences Education, Universitas Pendidikan Indonesia, Bandung, Indonesia

Article Info

Article history:

Received Mar 7, 2024

Revised Oct 30, 2024

Accepted Nov 19, 2024

Keywords:

Deflection

Ferrite core

Forces

Microactuators

Microelectromechanical systems

ABSTRACT

Microactuators play a vital role in several microelectromechanical systems (MEMS) that generate forces or deflections necessary to accomplish functions such as scanning, tuning, manipulation, or delivery. Utilizing a ferrite magnetic core has shown the potential to enhance the deflection of the microactuator. However, the previous study presented a complex fabrication method with high power consumption unsuitable for micropump application. Herewith, we report the impact of ferrite core length on the deflection generated by a microactuator with a simple fabrication method. The deflection behavior shows that the corresponding magnetic core length is inverse to the deflection improvement. The force reduction generated led by a longer magnetic core because of the farther distance to the coil. Our study can be used as a reference to support the development of micropump or active micromixer devices, which require compact devices with simple fabrication and high deflection, achieving ultra-high flow rate and high mixing index.

This is an open access article under the [CC BY-SA](#) license.



Corresponding Author:

Roer Eka Pawinanto

Study Program of Industrial Automation Engineering Education and Robotics

Faculty of Engineering Education and Industry, Universitas Pendidikan Indonesia

St. Dr. Setiabudi No. 207, Isola, Sukasari, Bandung 40154, West Java, Indonesia

Email: roer_eka@upi.edu

1. INTRODUCTION

The miniaturization of tools for in vivo diagnosis and surgical procedures has achieved remarkable advancements, significantly enhancing minimally invasive medicine in areas of the body with limited space [1]. This progress is exemplified by the compact and safe tools that have been developed, such as forceps and endoscopes, and are continuously refined to better address patient needs [2]. As medical technology evolves, the demand for advanced components that can further optimize these tools becomes increasingly critical. In this context, membrane microactuators play a vital role as integral components within

microelectromechanical systems (MEMS), offering widespread applications, including in micropumps [3]. These microactuators are essential for achieving the precision and functionality required in miniature medical devices. A range of membrane microactuators has been developed, utilizing various actuation mechanisms such as the piezoelectric (PZT) effect [4], shape memory alloy (SMA) effect [5], and electromagnetic (EM) forces [6]. While PZT membrane actuators are known for their rapid response times and substantial driving forces, they often require high driving voltages, limiting their integration into compact devices [7]. Although capable of significant deflections, SMA membrane actuators face challenges such as slow response times and reduced effectiveness in applications requiring rapid heat dissipation, such as pump mechanisms [8].

In contrast, EM actuation offers notable advantages, including the ability to generate substantial magnetic forces and high-frequency oscillations, making it a highly effective choice for microactuators [9]. Additionally, the power consumption of EM actuators, ranging from 13 milliwatts to 7 watts, underscores their potential for optimized performance in miniaturized medical tools [10]. Therefore, the ongoing development of MEMS technology and microactuators is crucial for advancing the capabilities of these sophisticated medical devices.

A compact micropump typically consists of an EM membrane microactuator comprising three main components: a flexible membrane, a permanent magnet, and a magnetic field generator [11]. Several previous studies have explored various EM actuation methods. For instance, Said *et al.* [12] developed an EM actuation method by fabricating a bonded magnet on a polydimethylsiloxane (PDMS) substrate, achieving a deflection of 9.16 μm . However, this method was constrained by the low aspect ratio of 0.03, which resulted in reduced driving force due to low packing density and self-demagnetization [12]. Ni *et al.* [13] investigated a PZT actuator in their micropump, achieving a maximum vibration amplitude of 29.4 μm . While previous studies investigated the impact of PZT and electroactive polymers (EAPs), they did not explicitly address the influence of material selection and structural configuration on optimizing deflection and force output. Gu *et al.* [14] utilized an ionic EAP in their microactuator array, achieving a displacement variation of 67 μm . However, the long-term stability of EAPs under continuous operation remains a concern [14]. Zhou *et al.* [15] used a thin NdFeB magnet enclosed within a PDMS membrane, recording a maximum deflection of 34.34 μm . Qi *et al.* [16] developed a MEMS-based EM membrane actuator with a maximum deflection of 100 μm , demonstrating substantial force and compact design. However, these studies did not explore the combined effects of magnetic field configuration and material properties in enhancing compact micropumps' deflection capabilities and operational reliability. This study addresses these gaps by investigating these factors to improve deflection efficiency and long-term durability of the micropump's membrane actuator.

Therefore, in this study, the impact of ferrite core length on the deflection of the microactuator is investigated. The fundamental principle of EM actuation involves the interaction between a permanent magnet composed of NdFeB material and a magnetic field generator, generating a magnetic force. The magnetic field generator consists of a ferrite core surrounding a copper wire, which displays variations in lengths of the ferrite core and varying numbers of coils through which an electric current can be generated. We found that the deflection of the microactuator correlates strongly with the length of the ferrite core. Longer ferrite cores tended to produce higher deflections due to the increased magnetic flux density. Additionally, the proposed method in this study showed that microactuators with ferrite core lengths of 10 mm or more had a disproportionately higher deflection than those with shorter cores due to enhanced EM interaction.

2. METHOD

The structure of the ferrite magnetic core-based microactuator is presented in Figure 1. The actuator comprises a flexible membrane, permanent magnet, and magnetic field generator. The design of the microactuator was created and simulated using COMSOL Multiphysics 6.0, employing studies in magnetic fields and solid mechanics to analyze the performance and interaction of the components. In Figure 1, D_m , h_m , and T_m are the diameter, height, and thickness of the membrane; L_f and D_f are the length and the diameter of the ferrite core; W_s , L_s , and T_s are the width, length, and thickness of the substrate, and D_{pm} is the diameter of the permanent magnet. The various dimensions of the ferrite magnetic core microactuator used are shown in Table 1. The permanent magnet is circular and placed in a membrane made from NdFeB with a diameter of 2 mm and a thickness of 1 mm. The magnetic field generators are made from ferrite cores with varying lengths wrapped around the copper wire with varying numbers of turns [17]. It is located at the bottom of the membrane with a distance of 1 mm. The center of the coil wire is precisely aligned with the magnet's edges to achieve the most significant vertical force [18]. An investigation into the influence of the number of magnets and coil cross-section on the actuating force is carried out to determine the arrangement with the best actuator performance [19]. The ferrite magnetic core microactuator is improved by the parameters and values shown in Table 2. Several parameters are used, such as the input current (I), number of turns of the coil (N), length of ferrite core (L_f), and distance coil to a permanent magnet (x). The parameters are chosen because they can generate the deflection of flexible membranes.

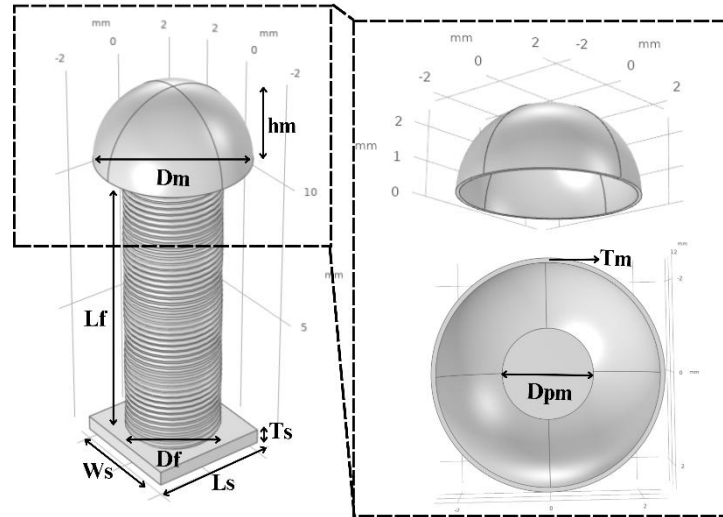


Figure 1. Configuration of the ferrite magnetic core-based microactuator

Table 1. Geometric dimensions of the microactuator in millimeters (mm)

D_m	h_m	T_m	L_f	D_f	W_s	L_s	T_s	D_{pm}
5	3	0.1	10, 5, 4, 2	3	5	5	0.1	2

Table 2. Parameters and value of microactuator

Parameter	Value
Input current (I)	0.2 A, 0.4 A, 0.6 A, 0.8 A, and 1.0 A
Number turns of coil (N)	25, 50, 75, and 100
Length of ferrite core (L_f)	10 mm, 5 mm, 4 mm, and 2 mm

The actuation principle is determined by structural dimension, response time, torque, maximum power consumption, technology used, and applied forces. The forces are divided into two categories: external forces and internal factors. EM actuators are classified as external forces since the forces are generated by the interplay of magnetic fields in the space between the stationary and moving elements [20]. In general, magnetic membrane actuation is accomplished through the deformation of the movable membrane caused by the generated magnetic force acting on the membrane [21].

A vertical magnetic force operating on the magnetic membrane with vertical magnetization on the z -axis is formed by the interaction of a magnet and an EM coil [22]. The magnetic force, often known as the Lorentz force (F_L) is given by the magnetic remanence (B_r), the cross-sectional area (A_m), and the integral of the distance between the permanent magnet and the membrane (h_m) with the z -axis [23]:

$$F_L = B_r A_m \int_z^{h_m} \frac{\partial H_z}{\partial z} dz \quad (1)$$

From (1), it can be seen that the pressure (P_o) value exerted by dividing the EM force (F_L) by the cross-sectional area (A_m) shown in (2).

$$P_o = \frac{F_L}{A_m} \quad (2)$$

Material characteristics of the membrane (D) that is defined by [24]:

$$D = \frac{E t_m^2}{12(1-\nu^2)} \quad (3)$$

where E denotes the Young's modulus, ν the Poisson's ratio, and t_m the membrane thickness. Ferrite core EM coil wires are attached to the movable membrane surface. When an electrical current is applied to the ferrite core coil wires, the permanent magnet induces magnetic flux onto the wires. The magnetic force (F_L) is generated and acts on the membrane as a result of this induction, resulting in the periodic actuation of the membrane structure. The actuating membrane is called deflection (W_{max}) which can be expressed as [25]:

$$W_{maks} = \frac{P_o a^2}{32 D} \quad (4)$$

From (4), the maximum deflection (W_{max}) can be seen with P_o being the applied pressure, a is the radius of the membrane, and D is the material characteristics of the membrane.

The fabrication process includes membrane fabrication and magnetic field generator fabrication. Firstly, it is important to consider the various stages involved in membrane fabrication. The selection of PDMS as the material for developing the membranes was based on its advantageous characteristics, including its simplicity of production and its ability to maintain optical transparency. In comparison to silicone, this substance has a lower cost. The manufacturing process begins with fabricating a primary mold using a glass rod. The master mold utilized in this context is constructed using glass domes. The master glass mold gets a cleaning process involving acetone, followed by rinsing with DI water and drying with N₂. The master mold is submerged in a solution of poly acrylic acid (PAA) and subsequently placed for a drying process on a hotplate for 10 minutes to facilitate the removal of the device from the master mold [26]. During 10 minutes, the PDMS and curing agent are combined and subjected to agitation. Subsequently, the mixture is placed in a desiccator for 30 minutes to remove any trapped air bubbles. In addition, PDMS is applied to the master mold to generate spacers. It is subjected to a heating process for 20 minutes on a hot plate maintained at a temperature of 100 °C to enhance the stability of the spacer [27]. In addition, PDMS is introduced into the system to form the membrane, which is subsequently subjected to centrifugation for 50 seconds at a speed of 500 revolutions per minute. The method described involves subjecting the sample to a temperature of 100 °C on a hot plate for 10 minutes [28]. The results of the membrane fabrication are depicted in Figure 2(a). The second step involves the fabrication of a magnetic field generator utilizing a ferrite core and coiling. Initially, the ferrite core should be measured with lengths of 10 mm, 5 mm, 4 mm, and 2 mm. Once the ferrite core has been appropriately sized, it is necessary to fabricate a support (also referred to as a substrate) using a thin glass material with a thickness measuring 0.5 mm. The coil is fabricated using copper wire with 25, 50, 75, and 100 turns, respectively. The diameter of the copper wire is 0.3 mm. The magnetic field generator is installed between the membrane, maintaining a separation distance of 1 mm. The results of the fabrication of the ferrite magnetic core are presented in Figure 2(b).

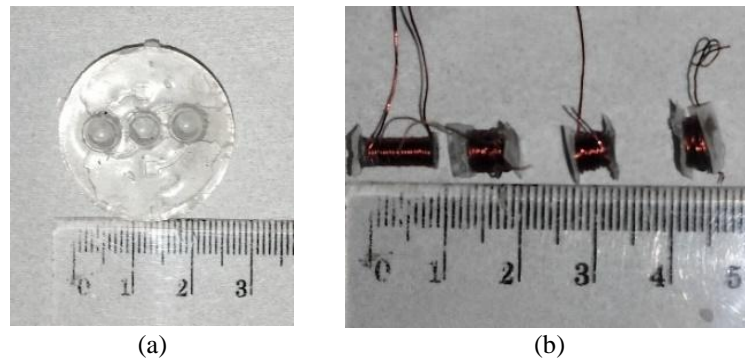


Figure 2. Fabrication result; (a) membrane and (b) ferrite magnetic core

A laser deflection meter (LDM) can measure the maximum deflection measurement. The laser deflection sensor ranging principle involves the utilization of triangulation, wherein the emission element and the position-sensitive device (PSD) are combined to carry out ranging, which entails deflection detection [29]. The laser deflection sensors that emit light utilize a semi-conductor laser. The emitting lens directs and concentrates the laser light before being projected onto a membrane. During that period, a portion of the light beam reflected from the object generates a luminous spot on the position-sensing device. The deflection of the PSD is observed to correspond with the movement of the object [30]. The ability to detect changes in positions enables the detection of membrane deflection. Certain receiving elements utilize a linear image sensor instead of the PSD. The PSD allows for acquiring information solely about the central position of the overall light spot's intensity.

In contrast, in conjunction with the linear image sensor, the emitting elements detect the quantity of light each cell receives. Hence, despite potential fluctuations in light levels caused by the object's surface characteristics, achieving enhanced precision in detecting the highest point of light intensity is still possible. This phenomenon significantly reduces errors resulting from the impact of the surfaces of the objects.

3. RESULT AND DISCUSSION

3.1. Simulation result

The models of ferrite magnetic core-based microactuators with dimension parameters and material properties are listed in Tables 1 and 2. Meanwhile, simulation results of deflection with input current 0.2 A, 0.4 A, 0.6 A, 0.8 A, and 1.0 A are shown in Figure 4. It suggests that the applied input significantly affects the membrane's deformation capability. Applying a higher input current leads to an increase in the deflection height, which produces a greater force.

Nevertheless, it is necessary to consider the issue of low power consumption in light of the potential damage to the membrane caused by the heating effect of the micro-coil [31]. The deflection results of a simulation are examined using a ferrite core with a length of 10 mm. The input current varies at 0.2 A, 0.4 A, 0.6 A, 0.8 A, and 1.0 A. The number of coils also varies at 25, 50, 75, and 100 levels. The maximum deflection value (W_{max}) is achieved when a current of 1.0 A is passed through a copper wire consisting of 100 turns, resulting in a deflection of 32.2 μm .

The core length is modified to 5 mm to investigate the impact of varying the length of the ferrite core. The change is made by maintaining the input current parameters and the number of coil changes. In the context of ferrite cores, it can be observed that a decrease in core length corresponds to an increase in either winding thickness or outer radius. The maximum deflection (W_{max}) value of a ferrite core with a length of 5 mm occurs when a current of 1.0 A is applied through 100 turns of copper wire, resulting in a deflection of 60 μm . The ferrite core has a length of 4 mm. Under the same input current parameters and number of coil turns, the maximum deflection (W_{max}) is observed to be 140 μm when the current is 1.0 A with 100 turns of copper wire. The optimal performance is achieved when the ferrite length is set to 2 mm while keeping the input current parameters and number of coils turns constant. This configuration led to a significantly thicker winding. The value of maximum deflection (W_{max}) reached 110.1 μm .

This study successfully investigated the impact of frequency resonance on the resultant deflection magnitude, with data for frequencies ranging from 1 kHz to 2 kHz and a 1.0 V excitation illustrated in Figure 3. The findings reveal distinct patterns in deflection across these frequencies. Specifically, Figure 3(a) shows the deflection pattern at 1.0175 kHz, where the deflection is relatively low. Figure 3(b) depicts the deflection at 1.4044 kHz, showing moderate deflection levels. At 1.6165 kHz, illustrated in Figure 3(c), the device achieves a maximum deflection of 10 μm , indicating that the device reaches a threshold where heat dissipation becomes inadequate for effective cooling. Figures 3(d) and (e) present the deflection at 1.6692 kHz and 1.7764 kHz, respectively, where deflection values become insufficient at higher frequencies. Thus, the study demonstrates that reversible partial heating and cooling are feasible within the given time scales. However, the response is not entirely symmetrical throughout the actuation cycle, as the cooling response, governed by surface-free convection, is slower than the heating response associated with volumetric Joule heating [30].

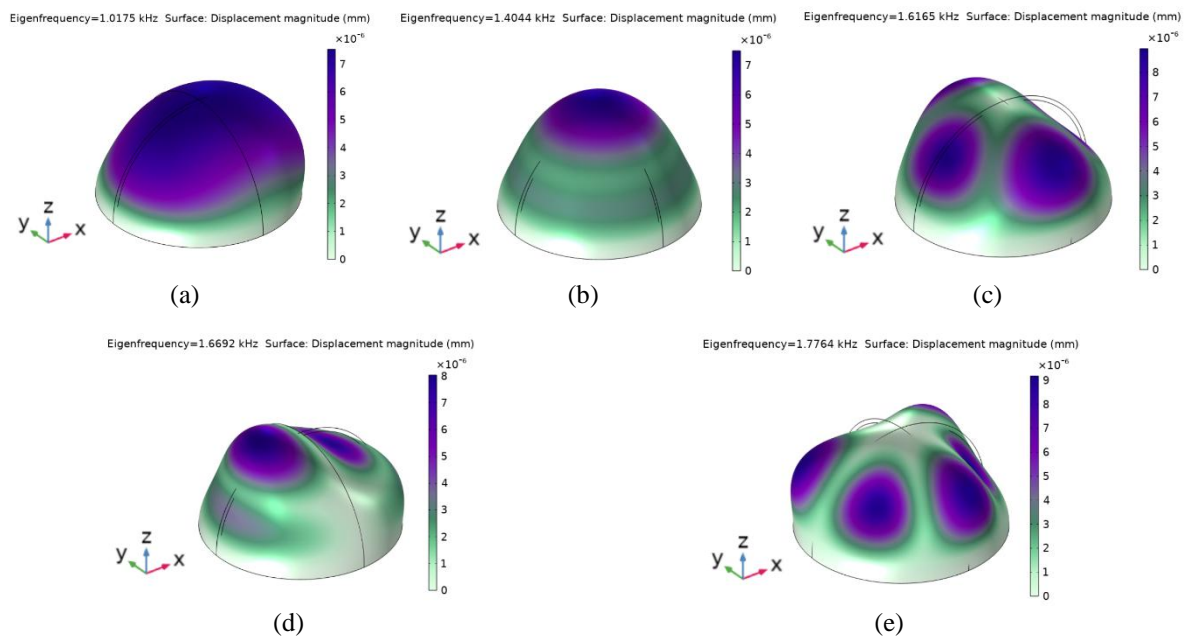


Figure 3. Various frequency resonance effects of PDMS membrane material; (a) 1.0175 kHz, (b) 1.4044 kHz, (c) 1.6165 kHz, (d) 1.6692 kHz, and (e) 1.7764 kHz

3.2. Experimental result

The experimental configuration used to determine the properties of the actuator comprises a LDM for quantifying the vertical deflection of the membrane positioned perpendicular to the deforming surface of the membrane. Additionally, a Gauss meter is utilised to measure the intensity of the magnetic field density generated by the EM coil and a power supply. The experimental deflections are compared and presented in Figure 4. The length of the ferrite core is 10 mm, and the input current values are 0.2 A, 0.4 A, 0.6 A, 0.8 A, and 1.0 A. Figure 4(a) depicts the number of coil revolutions for 25, 50, 75, and 100 values. The maximum deflection value (W_{max}) is achieved when a current of 1.0 A is provided through a copper wire with 100 turns, resulting in a deflection of 34.1 μm . The result indicates that the maximum deflection (W_{max}) exceeds the simulated value, specifically measuring 32.4 μm .

The length of the ferrite core was changed to 5 mm to determine the effect of changing the length of the ferrite core with the same input current parameters and number of coil revolutions. The shorter the ferrite core, the thicker the winding or the larger the outer radius. As shown in Figure 4(b), it produces the maximum deflection (W_{max}) value when the current is 1.0 A and 100 turns of copper wire, namely 62.2 μm , compared with the simulation, which produces a maximum deflection (W_{max}) of 60 μm . A ferrite core length of 4 mm with the same input current parameters and number of coil turns shows results in Figure 4(c), namely the maximum deflection (W_{max}) value when the current is 1.0 A and 100 turns of copper wire is 150.2 μm , compared with the simulation results, namely 140 μm . The best performance was obtained at a ferrite length of 2 mm with the same input current parameters and number of coil turns, resulting in a much thicker winding. The maximum deflection (W_{max}) value reached 168.4 μm compared to the simulation result of 110.1 μm . The comparison between the simulation and measurement results shows that the simulation results reveal a higher value than that from the measurement. This higher value is possibly due to the ideal case considered in the simulation parameter. On the other hand, several lost factors in the measurement process, such as inner resistance on the Gauss meter and power supply, reduce the measurement precision [31].

The experimental configuration used to determine the properties of the actuator comprises a LDM for quantifying the vertical deflection of the membrane positioned perpendicular to the deforming surface of the membrane. Additionally, a Gauss meter and a power supply are utilized to measure the intensity of the magnetic field density generated by the EM coil. The experimental deflections are compared and presented in Figure 4. For the ferrite core length of 10 mm and various input current values (0.2 A, 0.4 A, 0.6 A, 0.8 A, and 1.0 A), the number of coil turns is depicted in Figure 4(a) for values of 25, 50, 75, and 100. The maximum deflection value (W_{max}) is achieved when a current of 1.0 A is passed through a copper wire with 100 turns, resulting in a deflection of 34.1 μm , as shown in Figure 4(a). This result indicates that the maximum deflection (W_{max}) exceeds the simulated value, specifically measuring 32.4 μm . The length of the ferrite core was changed to 5 mm to determine the effect of changing the core length with the same input current parameters and number of coil turns. The result is shown in Figure 4(b), where the maximum deflection (W_{max}) is 62.2 μm compared to the simulation result of 60 μm . For a ferrite core length of 4 mm, Figure 4(c) shows the maximum deflection (W_{max}) of 150.2 μm with 100 turns of copper wire, higher than the simulation value of 140 μm . The best performance was obtained at a ferrite length of 2 mm, as shown in Figure 4(d), with a maximum deflection (W_{max}) of 168.4 μm compared to the simulation result of 110.1 μm . The comparison between the simulation and measurement results shows that the results reveal higher values than the measured values, possibly due to ideal conditions considered in the simulation. At the same time, factors such as inner resistance in the Gauss meter and power supply contribute to the reduction of measurement precision [31].

The electrical and mechanical properties of the actuator were assessed to investigate the influence of coil parameters and input power on the deformation characteristics of the membrane. Applying an input current increases membrane deformation, which exhibits a positive correlation with the magnitude of the generated magnetic force. The utilisation of coil wire featuring a reduced cross-sectional area for current flow results in an augmented resistance within the coil, thereby leading to an increase in power consumption. Nevertheless, it is improbable that the increased cross-sectional area of the coil contributes to amplifying the magnetic field's generation, primarily due to the influence of the eddy current phenomenon [32]. Table 3 summarizes the maximum deflection values achieved in various EM and MEMS-based membrane actuator studies. This comparison highlights advancements in actuator performance over time and places our study's findings in context with previous research.

Our study, which utilizes a MEMS-based EM actuator with a ferrite core, achieves a maximum deflection of 168.4 μm , significantly higher than previous research. Our findings indicate that this higher deflection is not associated with poor performance in driving force or efficiency, as seen in earlier studies. While earlier studies demonstrated deflections ranging from 9.16 μm to 100 μm , our actuator's design enhancements and ferrite core integration have resulted in this notable improvement. The proposed method

benefits from the enhanced magnetic flux density of the ferrite core without negatively affecting the actuator’s operational stability or efficiency. This method showcases a substantial advancement in actuator performance compared to earlier studies. This study focuses on investigating various ferrite core lengths and input currents. Additional and in-depth research may be required to confirm the generalizability of these findings across different actuator designs and operational conditions, particularly regarding long-term stability and performance under varying environmental factors. Our research shows that the MEMS-based actuator with a ferrite core offers significant improvements in deflection compared to previous designs. Future research may explore various ferrite core materials and configurations and practical methods for optimizing actuator performance in real-world applications. Investigating the impact of environmental variables on actuator performance could also provide further insights into enhancing reliability and efficiency.

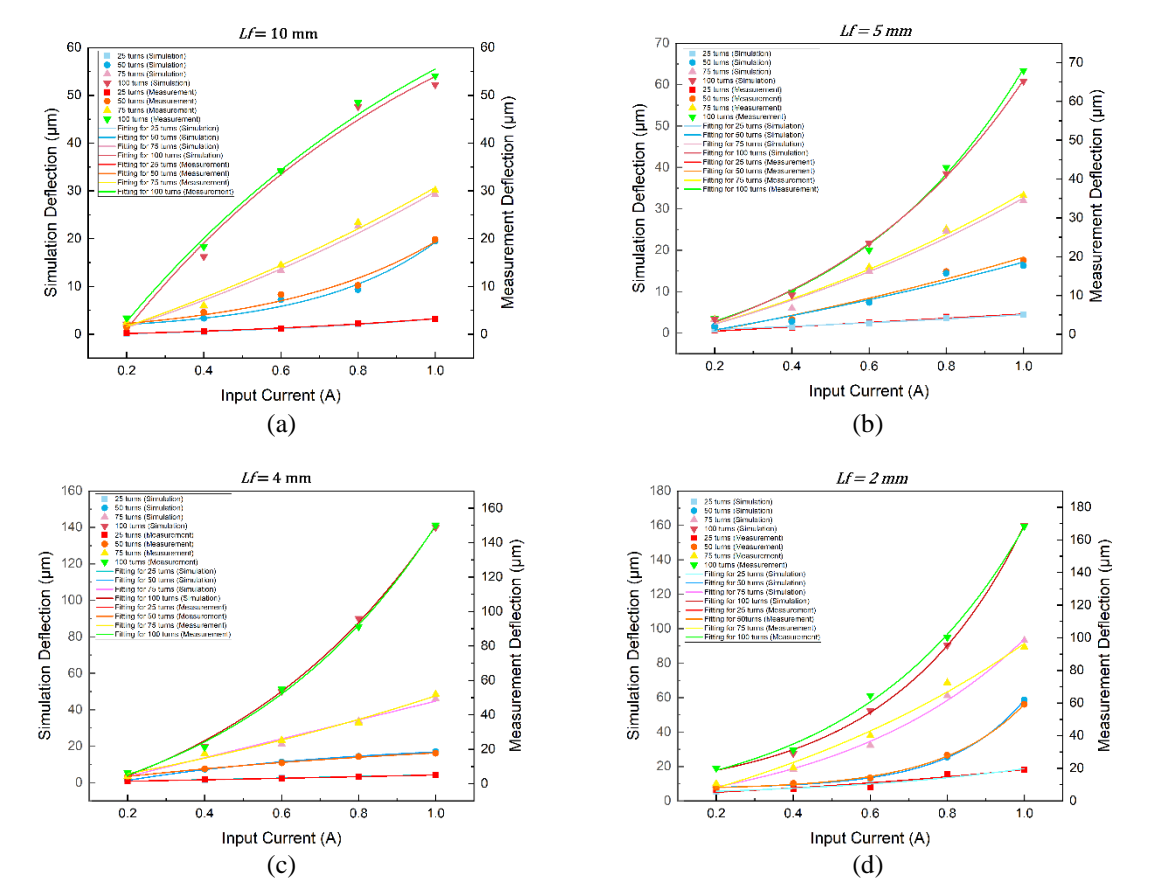


Figure 4. The deflection of simulation and experimental at ferrite core length; (a) L_f =10 mm, (b) L_f =5 mm, (c) L_f =4 mm, and (d) L_f =2 mm

Table 3. Comparison of maximum deflection values with previous research on EM and MEMS-based membrane actuators			
No	Reference	Structure	Maximum deflection (μm)
1	Our study	MEMS-based EM actuator with ferrite core	168.4
2	Said <i>et al.</i> [12]	Bonded magnet on PDMS substrate	9.16
3	Ni <i>et al.</i> [13]	PZT micropump	29.4
4	Gu <i>et al.</i> [14]	Ionic EAP microactuator array	67
5	Zhou <i>et al.</i> [15]	NdFeB magnet enclosed within a PDMS membrane	34.34
6	Qi <i>et al.</i> [16]	MEMS-based EM membrane actuator	100

4. CONCLUSION

In this study, we proposed and evaluated the concept of an EM membrane actuator based on MEMS utilizing a design method involving ferrite cores with varying lengths, coil turns, and input currents. Recent

observations indicate that the length of the ferrite core significantly impacts the actuator's deflection. Our findings prove that this phenomenon is linked to alterations in core length and coil configuration rather than being caused by simply increasing the number of coil turns or input current. The optimal result is achieved at a core length of 2 mm, 100 coil turns, and an input current of 1.0 A, resulting in a maximum deflection of 168.4 μm . Large deflection is crucial for the performance of microactuators because it allows the actuator to produce significant changes in volume or flow in applications such as micropumps and micromixers. Our findings contribute to a deeper understanding of how design parameters affect actuator performance and provide valuable guidance for further research and development.

ACKNOWLEDGEMENTS

The authors thank UPI and IMEN UKM for providing the simulation and experiment facility. This research was supported by funding from Universitas Pendidikan Indonesia with grant 528/UN40.LP/PT.01.03/2023, 1785/UN40/PT.01.02/2024 and program of World Class University 2021.




REFERENCES

- [1] S. Konishi and H. Kosawa, "High-output bending motion of a soft inflatable microactuator with an actuation conversion mechanism," *Scientific Reports*, vol. 10, no. 12038, pp. 1-10, Jul. 2020, doi: 10.1038/s41598-020-68458-5.
- [2] N. M. Kommanaboina, T. S. Yallew, A. Bagolini, and M. F. Pantano, "A C-shaped hinge for displacement magnification in MEMS rotational structures," *Microsystems & Nanoengineering*, vol. 10, no. 5, pp. 1-9, Jan. 2024, doi: 10.1038/s41378-023-00618-9.
- [3] A. Nisar, N. Afzulpurkar, B. Mahaisavariya, and A. Tuantranont, "MEMS-based micropumps in drug delivery and biomedical applications," *Sensors and Actuators B: Chemical*, vol. 130, no. 2, pp. 917-942, Dec. 2008, doi: 10.1016/j.snb.2007.10.064.
- [4] M. D. Nguyen, H. N. Vu, D. H. A. Blank, and G. Rijnders, "Epitaxial $\text{Pb}(\text{Zr,Ti})\text{O}_3$ thin films for a MEMS application," *Advances in Natural Sciences: Nanoscience and Nanotechnology*, vol. 2, no. 2, pp. 2043-6262, Mar. 2011, doi: 10.1088/2043-6262/2/1/015005.
- [5] D. D. Shin, K. P. Mohanchandra, and G. P. Carman, "Development of hydraulic linear actuator using thin film SMA," *Sensors and Actuators A: Physical*, vol. 119, no. 1, pp. 151-156, Mar. 2005, doi: 10.1177/1045389X11414.
- [6] K. Nagai, N. Sugita, and T. Shinshi, "Influence of Permanent Magnetic Properties on Laser-Assisted Heating Magnetization for Magnetic MEMS," in *IEEE Access*, vol. 11, pp. 143446-143456, 2023, doi: 10.1109/ACCESS.2023.3341971.
- [7] M. S. Salem *et al.*, "Boosting the Electrostatic MEMS Converter Output Power by Applying Three Effective Performance-Enhancing Techniques," *Micromachines*, vol. 14, no. 2, pp. 485, Feb. 2023, doi: 10.3390/mi14020485.
- [8] C. R. Knick, "Optimization of MEMS actuator driven by shape memory alloy thin film phase change," *Advanced Functional Materials*, vol. 1, no. 1, pp. 72274, May. 2020, doi: 10.5772/intechopen.92393.
- [9] R. E. Pawinanto, J. Yunas, B. Y. Majlis, B. Bais, and M. M. Said, "Fabrication and testing of electromagnetic MEMS microactuator utilizing PCB based planar micro-coil," *ARPJ Journal of Engineering and Applied Sciences*, vol. 10, no. 8, pp. 8399-8403, Jan. 2015.
- [10] B. McIvor and J. Chahl, "Energy efficiency of linear electromagnetic actuators for flapping wing micro aerial vehicles," *Energies*, vol. 13, no. 5, pp. 1-17, Mar. 2020, doi: 10.3390/en13051075.
- [11] A. Subandi *et al.*, "A peristaltic electromagnetic (EM) micropump with dome-shaped PDMS membranes for biomedical application," *Sensors and Actuators A: Physical*, vol. 379, no. 1, p. 115942, Dec. 2024, doi: 10.1016/j.sna.2024.115942.
- [12] M. M. Said, J. Yunas, R. E. Pawinanto, B. Y. Majlis, and B. Bais, "PDMS based electromagnetic actuator membrane with embedded magnetic particles in polymer composite," *Sensors and Actuators A: Physical*, vol. 245, no. 1, pp. 85-96, Jul. 2016, doi: 10.1016/j.sna.2016.05.007.
- [13] J. Ni *et al.*, "Analytical and experimental study of a valveless piezoelectric micropump with high flowrate and pressure load," *Microsystems & Nanoengineering*, vol. 9, no. 1, pp. 72, Jun. 2023, doi: 10.1038/s41378-023-00547-7.
- [14] J. Gu, Z. Zhou, Y. Xie, X. Zhu, G. Huang, and Z. Zhang, "A microactuator array based on ionic electroactive artificial muscles for cell mechanical stimulation," *Biomimetics*, vol. 9, no. 5, pp. 281, May. 2024, doi: 10.3390/biomimetics9050281.
- [15] B. Zhou *et al.*, "Design and fabrication of magnetically functionalized flexible micropillar arrays for rapid and controllable microfluidic mixing," *Lab on a Chip*, vol. 15, no. 9, pp. 2125-2132, Mar. 2015, doi: 10.1039/C5LC00173K.
- [16] C. Qi, D. Han, and T. Shinshi, "A MEMS-based electromagnetic membrane actuator utilizing bonded magnets with large displacement," *Sensors and Actuators A: Physical*, vol. 330, no. 1, p. 112834, Oct. 2021, doi: 10.1016/j.sna.2021.112834.
- [17] Y. Wang *et al.*, "A micro electromagnetic actuator with high force density," *Sensors and Actuators A: Physical*, vol. 331, no. 1, pp. 112771, Nov. 2021, doi: 10.1016/j.sna.2021.112771.
- [18] O. D. Oniku, B. J. Bowers, S. B. Shetye, N. Wang, and D. P. Arnold, "Permanent magnet microstructures using dry-pressed magnetic powders," *Journal of Micromechanics and Microengineering*, vol. 23, no. 7, pp. 1-19, Jun. 2013, doi: 10.1088/0960-1317/23/7/075027.
- [19] D.-S. Nicolescu, A. Radulian, C.-G. Saracin, and M. Maricar, "New Solution of High Force Linear Actuator with Permanent Magnets," *Revue Roumaine Des Sciences Techniques*, vol. 69, no. 2, pp. 165-170, Jun 2024, doi: 10.59277/RRST-EE.2024.2.8.
- [20] M. Uehara, "Microstructure and permanent magnet properties of a perpendicular anisotropic NdFeB/Ta multilayered thin film prepared by magnetron sputtering," *Journal of Magnetism and Magnetic Materials*, vol. 284, pp. 281-286, Dec. 2004, doi: 10.1016/j.jmmm.2004.06.047.
- [21] M. Nakano *et al.*, "Comparison of properties between Pr-Fe-B and Nd-Fe-B thick-film magnets applied to MEMS," *Japanese Journal of Applied Physics*, vol. 59, no. 1, pp. 1-17, Dec. 2019, doi: 10.7567/1347-4065/ab5534.
- [22] E. Pina *et al.*, "Coercivity in SmCo hard magnetic films for MEMS applications," *Journal of Magnetism and Magnetic Materials*, vol. 290-291, no. 2, pp. 1234-1236, Apr. 2005, doi: 10.1016/j.jmmm.2004.11.410.
- [23] Y. Zhang, D. Givord, and N. M. Dempsey, "The influence of buffer/capping-layer-mediated stress on the coercivity of NdFeB films," *Acta Materialia*, vol. 60, no. 9, pp. 3783-3788, May 2012, doi: 10.1016/j.actamat.2012.03.051.
- [24] T. P. Kumari, M. M. Raja, A. Kumar, S. Srinath, and S. V. Kamat, "Effect of thickness on structure, microstructure, residual




- stress and soft magnetic properties of DC sputtered Fe₆₅Co₃₅ soft magnetic thin films,” *Journal of Magnetism and Magnetic Materials*, vol. 365, no. 1, pp. 93–99, Sept. 2014, doi: 10.1016/j.jmmm.2014.04.030.
- [25] R. E. Pawinanto, J. Yunas, M. M. Said, M. M. Noor, and B. Y. Majlis, “Design and fabrication of PCB based planar micro-coil for magnetic MEMS actuator,” *2014 IEEE International Conference on Semiconductor Electronics (ICSE2014)*, Kuala Lumpur, Malaysia, 2014, pp. 487–490, doi: 10.1109/SMELEC.2014.6920904.
- [26] C. Song, P. Wang, and H. A. Makse, “Phase diagram for jammed matter,” *Nature*, vol. 453, no. 7191, pp. 629–632, May. 2008, doi: 10.1038/nature06981.
- [27] Hsien-Tsung Chang, Chia-Yen Lee, Chih-Yung Wen, and Boe-Shong Hong, “Theoretical analysis and optimization of electromagnetic actuation in a valveless microimpedance pump,” *Microelectronics Journal*, vol. 38, no. 6–7, pp. 791–799, Jul. 2007, doi: 10.1016/j.mejo.2007.04.013.
- [28] W. Sim, J. Oh, and B. Choi, “Fabrication, experiment of a microactuator using magnetic fluid for micropump application,” *Microsystem Technologies*, vol. 12, no. 9, pp. 1085–1091, Jul. 2006, doi: 10.1007/s00542-006-0130-2.
- [29] J. Xiang, Z. Cai, Y. Zhang, and W. Wang, “A micro-cam actuated linear peristaltic pump for microfluidic applications,” *Sensors and Actuators A: Physical*, vol. 251, pp. 20–25, Nov. 2016, doi: 10.1016/j.sna.2016.09.008.
- [30] O. Sahin, M. Ashokkumar, and P. M. Ajayan, “3 - Micro- and nanopatterning of biomaterial surfaces,” *Fundamental Biomaterials: Metals*, pp. 67–78, 2018, doi: 10.1016/B978-0-08-102205-4.00003-9.
- [31] P. K. Dey, B. Pramanick, A. RaviShankar, P. Ganguly, and S. Das, “Microstructuring of SU-8 resist for MEMS and bio-applications,” *International Journal on Smart Sensing and Intelligent Systems*, vol. 3, no. 1, pp. 118–129, Mar. 2010, doi: 10.21307/ijssis-2017-384.
- [32] S. Martin and B. Bhushan, “Transparent, wear-resistant, superhydrophobic and superoleophobic poly(dimethylsiloxane) (PDMS) surfaces,” *Journal of Colloid and Interface Science*, vol. 488, pp. 118–126, Feb. 2017, doi: 10.1016/j.jcis.2016.10.094.

BIOGRAPHIES OF AUTHORS






Roer Eka Pawinanto    is a senior lecturer at Universitas Pendidikan Indonesia. He is also a visiting research fellow at the Department of Physics, National University of Singapore. He received his Ph.D. in Electrical Engineering from Universiti Teknologi Malaysia under a Japan-ASEAN Integration Fund scholarship in 2020. He was awarded the top 10 of UPI's most productive researchers in the SCOPUS-based publication and the top 10 Hackathon [RE] energized Indonesia from UPI and New Energy Nexus Indonesia, respectively, in 2020. Moreover, he was awarded one of the top 10 IEEE Innovation Nation Indonesia in 2021. He has published two book chapters in electronics and more than 50 academic research papers. His work is focused on MEMS devices and technology for sensors and actuators, energy, and biomedical applications. He can be contacted at email: roer_eka@upi.edu.






Budi Mulyanti    a professor of material physics at the Faculty of Technology and Vocational Education (FPTK), Universitas Pendidikan Indonesia (UPI). She received Ph.D. in physics from Institut Teknologi Bandung, Indonesia in 2006. She is a senior member of the Institution of Electrical and Electronics Engineer (IEEE) since 2022. She is also a vice chairman of physics society of Indonesia Bandung Chapter. She is member of National Credit Assessment Team of Republic of Indonesia and also member of National Research Reviewer Republic of Indonesia. She was a head of Department of Electrical Engineering and Education FPTK UPI from 2015 until 2019. She was also head of TVET center FPTK UPI from 2008 until 2010. She was awarded as the best researcher from Universitas Pendidikan Indonesia in 2016. She has published three text books in material electronics for undergraduate courses and more than 80 academic research papers. Her current interests are design and fabrication of photonic devices, bioMEMS, and solar cell development. She can be contacted at email: bmulianti@upi.edu.






Jahril Nur Fauzan    received a bachelor's degree in Education from Electrical Engineering Education at the Universitas Pendidikan Indonesia in 2023. Currently working as a research assistant at the Universitas Pendidikan Indonesia. His research interest is photonic crystal cavities for telecommunication filter applications. Research and scientific publications that have been carried out include (1) The Optimization of Two-Dimensional Photonic Crystals Resonator (PCR)-based Filter for Telecommunication Applications, IEEE International Conference on Sensors and Nanotechnology (SENNANO), 2021; (2) Research trends related to photonic crystals (PHC) from 2009 to 2019: Bibliometric analysis and knowledge mapping, *Journal of Engineering Science and Technology*, 2022. Awards received include Top 10 IEEE Innovation Nation, 2021; First Winner International IoT Contest Asia Pacific Student Competition, 2022; and 1st Runner-up in the Indonesian Vocational Olympiad in the Control and Instrumentation Category for Industrial Sector, 2022. He can be contacted at email: jahrilnurfauzan@upi.edu.






Ayub Subandi    is an academic and researcher at Universitas Komputer Indonesia (UNIKOM), Bandung. He obtained his Master's degree from Institut Teknologi Bandung (ITB) and a Ph.D. from the Institute of Microengineering and Nanoelectronics (IMEN), Universiti Kebangsaan Malaysia (UKM). His research focuses on MEMS, microelectronics, nanoelectronics, sensors, and actuators, with an emphasis on biomedical applications. He has published numerous impactful studies, including advancements in electromagnetic micropumps, dome-shaped actuator membranes, and polymer-based MEMS for medical use. His contributions to micro- and nano-technology have been featured in high-ranking journals such as *Sensors and Actuators A: Physical* and *Polymers*, showcasing his dedication to innovation in biomedical engineering. He can be contacted at email: ayub.subandi@email.unikom.ac.id.



Lilik Hasanah    was born in Purworejo on June 16, 1977. In 1995, she was admitted to the Physics Department at ITB (Institut Teknologi Bandung) and graduated in 1999. She continued her studies for a Master's degree in the same department at ITB, completing it in 2001. In 2001, she became a lecturer in the Physics Education Department at FPMIPA, UPI (Universitas Pendidikan Indonesia), and was appointed as a civil servant. In 2003, she pursued a Ph.D. in the Physics Department at ITB, specializing in Computational Physics of Electronic Materials, supported by a scholarship from The Habibie Center Foundation. From 2009 to 2010, she participated in the DIKTI Academic Recharging Program, conducting collaborative research at the Department of Semiconductor Electronics and Integration Science, Graduate School of Advanced Sciences of Matter, Hiroshima University, Japan. Since 2008, she has been actively involved in numerous research collaborations with various institutions both nationally and internationally. These include BRIN (National Research and Innovation Agency), NCI, Hiroshima University, the Institute of Microengineering and Nanoelectronics (IMEN) at Universiti Kebangsaan Malaysia (UKM), the Department of Mechanical Engineering at Universiti Malaysia Pahang, the Faculty of Engineering at Universiti Malaysia Sarawak, the National University of Singapore (NUS), and many others. To date, she has produced 140 publications, encompassing both national and international scientific works, with a Scopus h-index of 10 and a Google Scholar h-index of 14, accumulating a total of 463 citations. She can be contacted at email: lilikhasanah@upi.edu.



M. Assadillah Pangestu    is the Director of Qrasa Utama Teknologi and the Chief Technology Officer (CTO) at Daya Propulsion International. He earned his Bachelor's degree in Electrical Engineering from Universitas Pendidikan Indonesia (UPI) in 2023. As Director of Qrasa Utama Teknologi, he oversees the development and implementation of innovative technology solutions, driving the company's growth in the tech industry. Concurrently, in his role as CTO at Daya Propulsion International, he specializes in Dynamic Positioning (DP) systems for offshore vessels, contributing to advancements in maritime technology. His expertise includes programming, computing, and website and server development, which he applies to enhance operational efficiency and safety in both fields. His technical acumen and leadership have established him as a prominent figure in technology and engineering. He can be contacted at email: reached at assadillahp@dp-indonesia.com or assadillahp@qrasa.co.id.



Jumril Yunas    is Assoc. Professor at the IMEN-UKM, Institute of Microengineering and Nanoelectronics, Universiti Kebangsaan Malaysia. He graduated in electrical engineering at the University of Technology RWTH Aachen, Germany and obtained his Ph.D. degree at the Universiti Kebangsaan Malaysia. He was Research Fellow at Indonesian Institute of Sciences, Indonesia and visiting scientist at the Chiba University, Japan. His work is focused in the area of MEMS device and technology for sensors and actuators, energy, and biomedical applications. He can be contacted at email: jumrilyunas@ukm.edu.my.